Three-Dimensional Structural Characterization of Centrosomes from Early *Drosophila* Embryos

Michelle Moritz,* Michael B. Braunfeld,‡ Jennifer C. Fung,‡ John W. Sedat,‡ Bruce M. Alberts,§ and David A. Agard‡

Department of Biochemistry & Biophysics and ‡Howard Hughes Medical Institute, University of California at San Francisco, San Francisco, CA 94143-0448

Abstract. An understanding of the mechanism and structure of microtubule (MT)-nucleating sites within the pericentriolar material (PCM) of the centrosome has been elusive. This is partly due to the difficulty in obtaining large quantities of centrosomes for analysis, as well as to the problem of attaining interpretable structural data with conventional EM techniques. We describe a protocol for isolating a large quantity of functional centrosomes from early *Drosophila* embryos. Using automated electron tomography, we have begun a three-dimensional structural characterization of these intact centrosomes with and without regrown MTs. Reconstructions of the centrosomes to ~6–8 nm resolution revealed no large structures at the minus ends of MTs, suggesting that if MT-nucleating material physically contacts the MTs, it must conform closely to the shape of the minus end. While many MTs originate near the centrioles, MT minus ends were found throughout the PCM, and even close to its outer boundary. The MTs criss-crossed the PCM, suggesting that nucleating sites are oriented in many different directions. Reconstructions of centrosomes without MTs suggest that there is a reorganization of the PCM upon MT regrowth; moreover, ring-like structures that have a similar diameter as MTs are apparent in the PCM of centrosomes without MTs, and may be MT-nucleating sites.

THE centrosome is the main nucleator of the microtubule (MT)[1] cytoskeleton in animal cells. The vital functions that the centrosome and its associated MTs participate in are remarkably varied and central to the life of the cell. During interphase, the centrosome and MTs contribute to the determination of cell polarity through their positioning of the endoplasmic reticulum and Golgi apparatus, as well as through their effects on the actin cytoskeleton. In mitosis, the centrosome and its associated MTs form the scaffolding of the spindle apparatus. At cytokinesis, the centrosome influences the placement of the cleavage furrow (reviewed in Kalnins, 1992; Kellogg et al., 1994).

The most basic function of the centrosome is to nucleate MTs; although pure α- and β-tubulin heterodimers can polymerize into MTs in vitro, this requires high tubulin concentrations. In vivo, most or all MTs are thought to grow from the centrosome, primarily because of the kinetic barrier to spontaneous nucleation. The number, length, and stability of the MTs emanating from the centrosome varies with the cell cycle. During interphase, there are relatively few MTs, and they are long and relatively stable. In mitosis, many more MTs are nucleated, and they are shorter and show an increased frequency of transition from growing to shrinking. These cell cycle-dependent changes in the properties of MTs are thought to be controlled by cyclins and their dependent protein kinases, some of which have been shown to localize to centrosomes at particular points in the cell cycle (reviewed in Kellogg et al., 1994).

The centrosome consists of a pair of centrioles, which are cylindrical arrangements of MTs, surrounded by a complex collection of proteins known as the pericentriolar material (PCM) or centrosome matrix (Kalnins, 1992; Kalt and Schliwa, 1993; Kellogg et al., 1994). The PCM has long been known to be the part of the centrosome that is responsible for MT nucleation (Gould and Borisy, 1977), but the mechanistic details remain largely unknown.

One approach has been to use electron microscopy (EM) to search for structural clues within the PCM that might suggest how MT nucleation is accomplished; but the apparently random, amorphous arrangement of the nucleating material does not readily suggest a mechanism (reviewed in Kalnins, 1992). There is good evidence suggest-

Dr. Alberts' present address is National Academy of Sciences, 2101 Constitution Ave. NW, Washington, DC 20418.

Address all correspondence to Michelle Moritz, Dept. of Biochemistry & Biophysics, University of California at San Francisco, San Francisco, CA 94143-0448. Tel.: (415) 476-4581. Fax: (415) 476-0806.

1. *Abbreviations used in this paper*: MT, microtubule; PCM, pericentriolar material.

ing that there are a limited number of MT-nucleating sites within the centrosome (Brinkley et al., 1981; Byers et al., 1978; Kuriyama, 1984; Mitchison and Kirschner, 1984). These sites can be thought of as subunits of the PCM (Kellogg et al., 1994); they determine the number of protofilaments in the MTs, possibly by acting as templates (Tilney et al., 1973; Scheele et al., 1982; Evans et al., 1985).

Another approach to understanding how the PCM nucleates MTs has been to characterize the proteins within it. Although a number of centrosomal proteins have been identified in a variety of organisms (reviewed in Kalt and Schliwa, 1993; Kellogg et al., 1994), currently, γ-tubulin is the only protein to be strongly implicated in MT nucleation (Oakley et al., 1990; Horio et al., 1991; Stearns et al., 1991; Joshi et al., 1992; Felix et al., 1994; Stearns and Kirschner, 1994). This highly conserved tubulin variant is localized exclusively to the centrosome, and the current hypothesis is that it interacts directly with the minus ends of MTs (reviewed in Oakley, 1992). However, γ-tubulin exists inside cells as part of a larger protein complex (Raff et al., 1993; Stearns and Kirschner, 1994), suggesting that there may be other centrosomal proteins involved in MT nucleation as well.

Although centrosomes have been studied extensively by electron microscopy (reviewed in Kalnins, 1992; Wheatley, 1982) no ordered structure within the PCM has been discernible, and the structure of the MT-nucleating site remains undefined. Historically, serial, thin-section EM has been used to visualize the centrosome (e.g., Wheatley, 1982; Alieva et al., 1992; Rattner, 1992). While this approach has provided some information about the centrioles and MT-nucleating material, it has not produced high resolution details, perhaps because it is relatively rare that perfectly transverse or longitudinal sections through a given structure are obtained. In addition, the loss of tissue between sections, the potential variation in section thickness, uneven compression, and material loss upon exposure to the electron beam are problems encountered in conventional serial sectioning (reviewed in Bozzola and Russell, 1992).

More recently, electron microscopic tomography has been employed to visualize and interpret complex biological structures (Olins, 1986; Skoglund et al., 1986; Belmont et al., 1987; Frank et al., 1987; McEwen et al., 1993). Tomography is a technique whereby a three-dimensional object is reconstructed from a set of tilted projections (reviewed in Frank, 1992). Because all of the data is collected from a single specimen, no prior assumptions regarding sample crystallinity or symmetry need to be made.

Although extremely powerful, EM tomography has not been widely used because of significant practical difficulties. A large number of tilted views (~120) must be taken at fine tilt intervals (~1.25° covering the range ± 70°). Because of the inability to make the sample perfectly eucentric, the specimen will precess as it is tilted (changing both x-y position and focus) necessitating constant recentering and refocusing. Each of the resultant images must be digitized, precisely aligned with one another and converted to be proportional to specimen mass, and finally reconstructed.

Recently, the laboratories of Agard and Sedat have been able to dramatically simplify this process. A large-format charge-coupled device detector allows direct digital image acquisition and eliminates the need for recoding images on film and subsequent digitization. More importantly, the combination of on-line image acquisition with real-time computer control of the electron microscope permits the data collection process to be fully automated (Koster et al., 1992, 1993). After each tilt, the image is electronically recentered and refocused. In addition to greatly simplifying the task of collecting three-dimensional EM data, the total exposure to the electron beam can be reduced 100–1,000-fold; further improving reconstruction quality. Data analysis methods have also been greatly streamlined, so that producing three-dimensional reconstructions is now a simple, straightforward procedure. These improvements should greatly improve the accessibility of this powerful technique to the cell biology community.

Here we describe the isolation of functional centrosomes from early *Drosophila* embryos, and their use to begin a detailed structural characterization of the MT-nucleating site using electron tomography.

Materials and Methods

Isolation of Centrosomes from Embryos

Collections of 0–3.5 h Oregon R embryos (7–40 g) were dechorionated in 50% bleach for 2 min, rinsed in distilled H_2O, blotted dry, and then Dounce homogenized (five passes) in the cold room in 5 vol (wt/vol) ice-cold Buffer 1 (80 mM Potassium-Pipes, pH 6.8, 1 mM Na_2EGTA, 1 mM $MgCl_2$, 100 mM KCl, 14% sucrose (wt/vol, ultrapure; ICN, Aurora, OH), and protease inhibitors (1 mM PMSF, 10 μM benzamidine-HCl, 1 μg/ml phenanthroline, 10 μg/ml aprotinin, 10 μg/ml leupeptin, and 10 μg/ml pepstatin A). Buffers 1 and 2 (see below) were prepared from a 5× stock containing 400 mM potassium-Pipes, pH 6.8, 5 mM Na_2EGTA, 5 mM $MgCl_2$, to which the other ingredients were added. The homogenate was filtered twice through wet Miracloth (Calbiochem Novabiochem, La Jolla, CA), and then centrifuged at 1500 *g* twice for 10 min. Floating lipids were aspirated off and the homogenate was transferred to a new tube between centrifugations. At this point, the supernatant was either frozen in liquid N_2 and stored at −80°C, or centrosomes were isolated from it immediately. The supernatant was brought to 0.1% or 0.5% in Triton X-100, and to 50% sucrose by adding 70% sucrose (wt/vol) in Buffer 2 (80 mM potassium-Pipes, pH 6.8, 1 mM Na_2EGTA, 1 mM $MgCl_2$, 100 mM KCl), and loaded onto a sucrose step gradient consisting of a 4 ml 55% step and a 3 ml 70% cushion (in buffer 2 plus 1 mM GTP). The gradients were centrifuged in an SW28 rotor (Beckman, Palo Alto, CA) at 100,000 *g* for 1.5 h. One 1-ml and seven 0.5-ml fractions were collected manually from each gradient in the cold room by puncturing the tube and allowing the gradient to drip from the bottom. Most of the centrosomes accumulate on top of the 70% cushion. They can remain on ice for several days, or frozen in liquid N_2 at −80°C and stored for many months with little loss of MT-nucleating activity.

Assay for MT Nucleation

MT-nucleating activity was tested by adding a mixture of rhodamine-labeled and unlabeled tubulin to centrosomes to a concentration of ~20 μM, incubating at 29°C for 10 min, and fixing in 10 vol 1% glutaraldehyde. The resulting asters were sedimented through a 30% glycerol cushion onto coverslips for viewing under the fluorescence microscope, as described previously (Mitchison and Kirschner, 1984; Evans et al., 1985).

Preparation of Tubulin

Since there was no apparent difference in the ability of *Drosophila* centrosomes to utilize tubulin purified from bovine brain or *Drosophila* (data not shown), we used bovine tubulin in all experiments. Bovine tubulin was purified as described previously, and cycled twice before use in aster regrowth experiments (Mitchison and Kirschner, 1984). Purified tubulin was

labeled with 5-(and-6-)carboxytetramethylrhodamine succinimidyl ester (Molecular Probes, Eugene, OR), as described previously (Hyman et al., 1991), and stored at −80°C in small aliquots.

Immunoblotting and Immunofluorescence

Immunoblots were performed as described previously (Kellogg and Alberts, 1992). Immunofluorescence on isolated centrosomes was performed as follows: asters were regrown from 4 μl (~80,000) centrosomes and rhodamine-labeled tubulin as described above and sedimented onto coverslips. Nonspecific binding of antibody was blocked by incubation of the coverslips in PBS (10 mM Na_2HPO_4, 1.8 mM KH_2PO_4, 136 mM NaCl, 2.6 mM KCl, pH 7.2), plus 5% BSA, 0.05% Tween-20, and 1 mM sodium azide (Block), for 20 min at room temperature. The coverslips were then incubated for 1 h at room temperature with primary antibody diluted in Block, washed 3 × 5 min in Block, incubated for 1 h in fluorescein-conjugated goat anti-rabbit antibody (or swine anti-goat antibody for CP190 staining) (Boehringer Mannheim Biochemicals, Indianapolis, IN), diluted 1:1,000 in Block, washed 3 × 5 min in Block, and mounted in 80% glycerol, 1 mg/ml *p*-phenylenediamine. Affinity-purified anti-CP190 goat polyclonal antibody, and anti-CP60 and anti-γ-tubulin rabbit polyclonal antibodies were each used at a concentration of ~1–2 μg/ml for Western blotting and immunofluorescence.

Electron Microscopy

Centrosomes with regrown asters were prepared for EM by incubating with pure bovine brain tubulin as described above. The asters were fixed in 10 vol of 1% glutaraldehyde (EM grade; Ted Pella, Inc., Redding, CA) in 80 mM Potassium-Pipes, pH 6.8, 1 mM $MgCl_2$, 1 mM Na_2EGTA, for 3–10 min, and sedimented at 23,000 *g* for 10 min through a filtered 30% glycerol cushion (in the same buffer) onto Thermonox disks (Nunc, Inc., Naperville, IL). Centrosomes without MTs were prepared in the same way, except the MT regrowth step was omitted. The asters or naked centrosomes were post-fixed in 1% OsO_4 in 0.1 M cacodylate, pH 7.4, for 10 min, and en bloc stained in 0.5% uranyl acetate in 30 mM veronyl acetate, pH 7.4, for 1 h in the dark. The material was subsequently dehydrated in ethanol and embedded by inverting the Thermonox disks onto Epon (Polysciences, Warrington, PA) using standard protocols (Hyatt, 1981). Semi-thick sections (0.7 μm) were cut with diamond knives (Diatome USA, Fort Washington, PA) using a Reichert Ultracut E ultramicrotome (Leica, Inc., Deerfield, IL). Sections were collected on formvar coated 50 × 200 mesh copper grids (Ted Pella, Inc.), and stained with uranyl and lead salts. Gold beads (15 nm; Amersham, Arlington Heights, IL), to be used as fiducial markers for alignment, were then applied to the section surface (Belmont et al., 1987). Sections were stabilized with a layer of evaporated carbon.

Tomographic data were collected for three centrosomes with MTs and three without using a Philips EM430 at 300 kV. The instrument is computer controlled using a Philips C400 interface. All data was recorded on a prototype Gatan 676 (Gatan, Inc., Pleasanton, CA) cooled (−30°C) slow-scan CCD camera (Photometrics, Inc., Tuscon, AZ) using a 1,024 × 1,024 pixel Thompson chip with 19 μm^2 pixels, 12 bit 200-kHz readout, and 20-μm thick YAG scintillator. Images were transferred from the camera into a Mercury 20-Mflops array processor (Mercury Computer Systems, Inc., Lowell, MA). A MicroVax III (Digital Equipment Corp., Maynard, MA) workstation was used for automated control of data collection and control of the instrument (Koster et al., 1993).

Automated data collection was accomplished as previously described (Koster et al., 1992, 1993). Data were collected at microscope magnifications of either 7.4Kx (3.84 nm/pixel at the CCD camera level) or 10.3Kx (2.78 nm/pixel). The sections were preirradiated before data collection (Braunfeld et al., 1994). Data were collected using an ultra-high-tilt stage (Gatan, Inc.). The data sets taken at 7.4Kx were collected over angular ranges of +70 to −75° and +75 to −65° at intervals of 1.25°. Data collected at 10.3Kx were collected over an angular range of +72.5 to −71.25° for centrosomes with MTs, and +65 to −65° for centrosomes without MTs, at 1.25° intervals.

The processing steps include alignment of the data stack, conversion of the measured image intensities into a measurement of mass density (mass normalization), and finally calculation of the reconstruction. Briefly, alignment of the data starts with identifying the positions of gold beads by employing an algorithm using a border walking scheme and size constraints to identify all bead-like features in each projection. This list of potential bead positions (determined to sub-pixel resolution) was compared to a manually determined list of bead positions allowing a subset (~10 beads) to be chosen for alignment (for details see Koster et al., 1993). The X and Y positions of the beads, as well as the rotation, translation, magnification, and shrinkage parameters, were determined by least squares analysis (Lawrence, 1983; D. N. Mastronarde, University of Colorado, Boulder, personal communication). The CCD image intensity data were next converted to mass densities, and corrected for variations in beam intensity and shutter timing. Background values (defined as that value for which only 1% of all pixels is higher) were estimated using intensity histograms on each image. Data were fitted using an exponential cosine curve modeling electron scattering in plastic sections at different tilt angles (∅). Each pixel was then converted into mass density using an exponential absorption model (Koster et al., 1993). Reconstructions were calculated using Resolution Weighted Back Projection (RWBP), Elliptical-square Weighted Back Projection (EWBP), or Tomographic Alternating Projection Iterative Reconstruction (TAPIR) algorithms (W. Liu, manuscript in preparation). Reconstructions were displayed and modeled using PRISM software (Chen et al., 1990, 1992).

Results

Isolation and Composition of Drosophila Centrosomes

Drosophila offers a number of advantages for dissecting the structure and biochemistry of the MT-nucleating sites at the centrosome. The early *Drosophila* embryo is very mitotically active, and the MT, actin, and chromosome dynamics of these early divisions can be readily followed in vivo using fluorescently labeled cytoskeletal proteins and histones (Kellogg et al., 1988; Minden et al., 1989). It is easy to obtain biochemical quantities of embryos, and because each embryo at the syncytial blastoderm stage is a single cell containing thousands of centrosomes, we reasoned that these embryos would be a good source for the biochemical isolation of these MT-organizing centers.

To isolate centrosomes, early embryos (0–3.5 h) are dechorionated and then homogenized (see Materials and Methods). This homogenate is filtered, and then centrifuged to remove nuclei and some yolk. The homogenate is separated on a sucrose step gradient; most of the centrosomes accumulate on top of the 70% cushion. MT-nucleating activity is tested using an assay in which rhodamine-labeled tubulin is added to the centrosomes and the resulting asters are centrifuged onto coverslips for viewing under the fluorescence microscope (Mitchison and Kirschner, 1984).

A typical yield from one 35-ml gradient (the equivalent of 2 g of embryos) is 1–5 × 10^7 functional centrosomes. The peak fraction (0.5 ml) contains ~5 μg of protein. This is roughly estimated to be a 10% yield (assuming an average of 2,500 centrosomes per embryo and that an embryo is 9.5 μg (Ashburner, 1989) and a 1,000-fold purification (based on the number of functional centrosomes per mg of protein in the starting homogenate compared to the same in the peak centrosome fraction). Greater than 90% of the centrosomes isolated are functional, as determined by comparing the number of regrown asters to the number of γ-tubulin-staining organelles in a microscope field (data not shown).

In the course of designing the centrosome isolation protocol, we tested the ability of various concentrations of Triton X-100 (0.1–0.5%) in the gradient load to prevent some of the abundant yolk from comigrating with centrosomes on the gradient. Interestingly, we found that in addition to separating much of the yolk (as well as other proteins) from centrosomes, the detergent has a clear ef-

fect on the composition of the centrosomes: the known centrosomal protein, γ-tubulin (Stearns et al., 1991; Zheng et al., 1991), is highly enriched in the centrosome-containing fractions regardless of the detergent concentration (fractions marked with asterisks in Fig. 1, *b* and *d*). CP190 (centrosomal protein of 190 kD, formerly known as DMAP190 or Bx63; Whitfield et al., 1988; Kellogg and Alberts, 1992) is somewhat enriched in centrosome-containing fractions, more so in the presence of 0.1% than 0.5% Triton X-100. However, CP60 (formerly known as DMAP60; Kellogg and Alberts, 1992), a centrosomal protein that was originally isolated based on its ability to form a complex with CP190, is only enriched in centrosome-containing fractions when 0.1% Triton X-100 is used. When the detergent concentration is increased to 0.5%, the majority of CP60 no longer comigrates with centrosomes (compare Fig. 1, *b* and *d*). Despite the fact that the composition of the centrosomes appears to be different under these two conditions, we see no gross differences at the light microscope level in the MT-nucleating activity of the two populations of centrosomes, suggesting that CP60 and any other proteins removed by 0.5% Triton X-100 are not required for the MT-nucleating activity of the centrosome (data not shown).

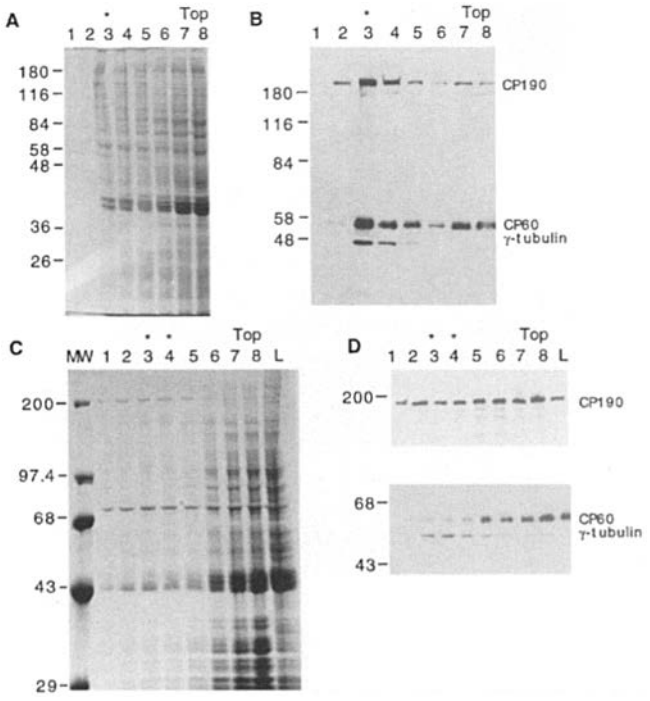

Figure 1. Protein profiles across centrosome gradients. Molecular weight markers are indicated on the left of each panel. Fraction numbers are at the top of each panel. For each gradient, one 1-ml fraction and seven 0.5-ml fractions were collected. Fraction 8 represents the top of the gradient. Asterisks mark gradient fractions containing the most centrosomes, as determined by aster formation. L indicates gradient load. (*a*) Coomassie-stained gel of proteins from fractions of a centrosome gradient containing 0.1% Triton X-100. ~20 μg protein were loaded per lane, except in lane *1*, where ~30 μl of fraction 1 were loaded. The peak fraction (*asterisk*) contained ~2×10^6 centrosomes. Fractions 1 and 2 contained virtually none. Fractions 4–6 contained ~10^4–10^5 centrosomes. (*b*) Immunoblot corresponding to gel in *a*. The blot was probed with antisera against CP190, CP60 and γ-tubulin, revealing that these proteins are enriched in fraction 3, which contains the most centrosomes. (*c*) Coomassie-stained gel of proteins from fractions of a centrosome gradient containing 0.5% Triton X-100. Because of the small amount of protein in each fraction, like fractions from three gradients were combined, diluted into 60 mM Tris, pH 6.8, 50 mM NaCl, 50 μg/ml insulin carrier protein, and concentrated. One-half of the protein obtained from fractions 1–5 was loaded. ~20 μg protein from fractions 6–8 were loaded. The peak fractions (*asterisks*) contained ~1×10^7 centrosomes. Fractions 1, 2, and 5–8 contained ~10^4–10^6 centrosomes. (*d*) Immunoblots corresponding to gel in *c*. The blots were probed with antisera against CP60 and γ-tubulin or CP190. In the presence of 0.5% Triton X-100, CP190 and γ-tubulin are still enriched in peak centrosome fractions, unlike CP60.

Immunofluorescence reveals that γ-tubulin is present at the centers of asters grown from isolated centrosomes (Fig. 2 *b*). Antibodies directed against CP190 give a similar staining pattern (data not shown). The CP60 antibodies stain some, but not all, centrosomes (data not shown). In addition, the region at the center of each aster stained by the antibody recognizing γ-tubulin varies in size, suggesting that different asters have different amounts of PCM (Fig. 2 *b*). These variations in size and composition may be due to cell cycle heterogeneity when the embryos were harvested, or they might reflect the isolation of centrosomes from embryos at somewhat different stages of development (Fig. 2).

Structural Analysis of Isolated Centrosomes

The ease of isolating large quantities of centrosomes from *Drosophila* embryos has allowed us to begin a detailed three-dimensional analysis of centrosome structure. Isolated centrosomes with regrown asters were prepared for electron microscopy by fixing in glutaraldehyde, sedimenting onto coverslips, staining with OsO_4 and uranyl acetate, and embedding in Epon (see Materials and Methods). Semi-thick (0.7 μm) sections were cut, collected on grids, and stained with uranyl and lead salts. Gold beads to be used as fiducial markers for alignment were then applied to the sections.

Four examples of "raw data" electron micrographs of centrosomes with regrown asters are shown in Fig. 2. As was suggested by the anti–γ-tubulin immunofluorescence (Fig. 2 *b*), different asters were found to contain different amounts of PCM (Fig. 2, *c–f*). The amount of PCM and the number of MTs is larger than is seen in typical isolated mammalian centrosomes, again suggesting that the *Drosophila* centrosomes were in mitosis upon isolation. Each aster contained one pair of centrioles, showing that the MT-nucleating material isolated is bona fide centrosomes.

To see structural detail within the PCM, it is necessary to do a tomographic reconstruction. The resolution of a tomographic reconstruction is dependent on the magnification (pixel size), the sample thickness, and the number and range of the tilted views. To maximize the resolution while still being able to visualize nearly an entire centrosome, we collected tilt data (Fig. 3) over a large angular range (± 70°), with a fine sampling interval (1.25°). We estimate that the final resolution is limited to ~6–8 nm, primarily by the low magnification used.

A series of selected images from the reconstruction

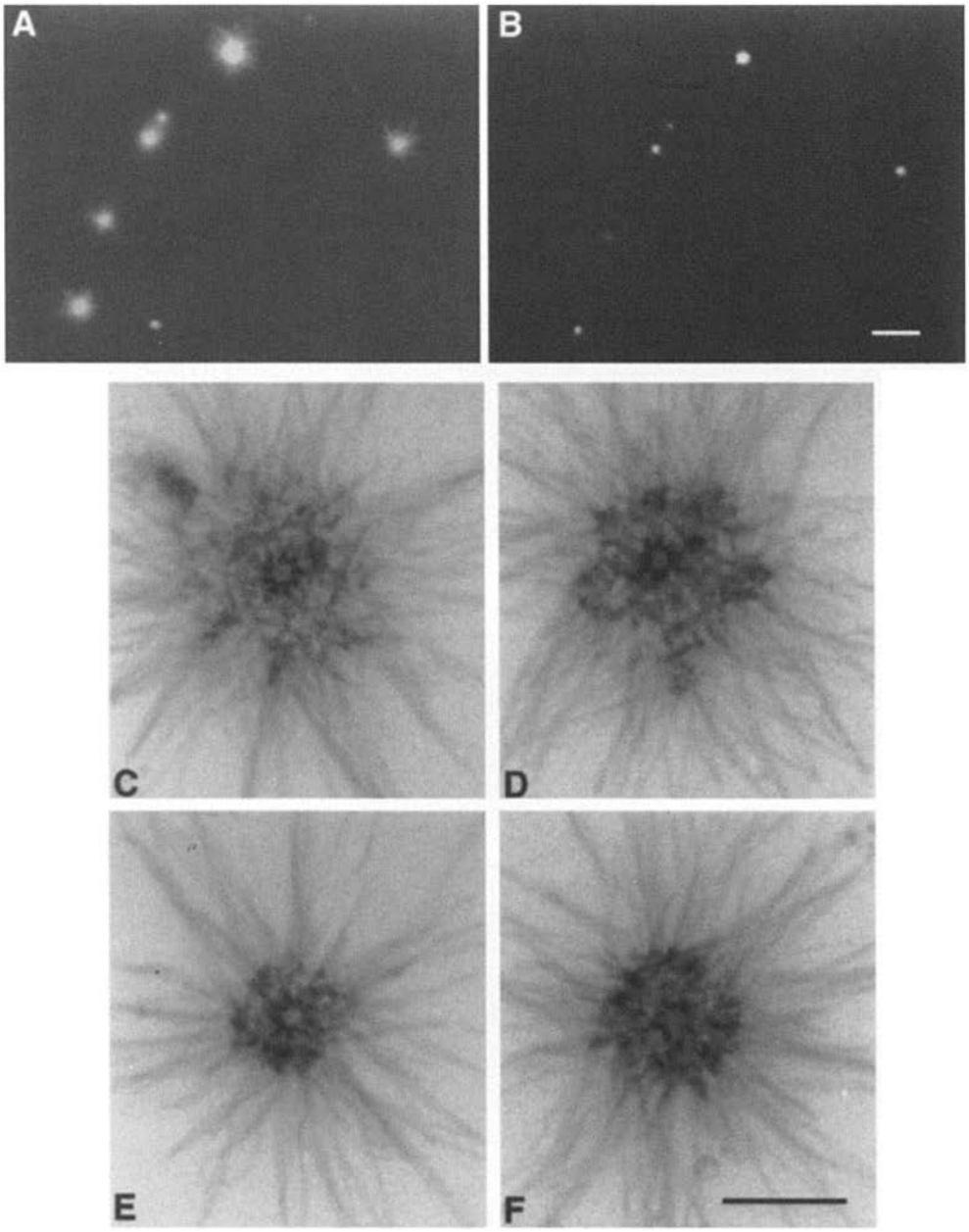

Figure 2. (*a* and *b*) Fluorescence light microscopy of isolated *Drosophila* centrosomes. (*a*) Isolated *Drosophila* centrosomes nucleate microtubules in vitro. Isolated centrosomes were incubated for 10 min at 29°C with a mixture of rhodamine labeled and unlabeled tubulin (final concentration ~20 μM). The sample was fixed in 0.1% glutaraldehyde and sedimented onto a coverslip. (*b*) γ-tubulin is associated with isolated *Drosophila* centrosomes. Immunofluorescence using γ-tubulin antiserum and a fluorescein-conjugated secondary antiserum was performed on the asters shown in *a*. (*c–f*) Electron tomography: examples of "raw data" from semi-thick (0.7 μm) sections of centrosomes with regrown microtubules. Note that different centrosomes contain different amounts of PCM, perhaps reflecting their cell cycle stage. Centrosomes with more PCM appear to nucleate more MTs (e.g., compare *c* with *e*). The centrosome in *c* was chosen for the reconstruction in Fig. 4. Bars: (*b*) 10 μm; (*f*) 500 nm.

(stepping through the centrosome) illustrates a number of important structural features (Fig. 4). The centrioles of the early *Drosophila* embryo consist of a ring of nine singlet MTs surrounding one central "tubule," whose appearance and dimensions suggest that it is a MT as well (see Discussion). The central tubule extends through the full length of the centriole (Fig. 4 *b*), and it appears to be connected to the outer ring by a series of nine radial "spokes." Electron-

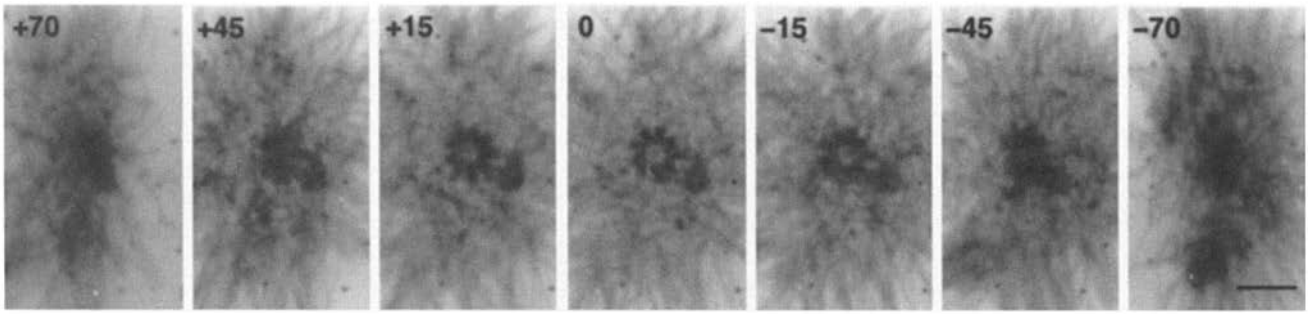

Figure 3. Tomographic data selected from a tilt series (+70 to −70°) to illustrate some of the raw data used for the centrosome reconstruction in Fig. 5. Bar, 200 nm.

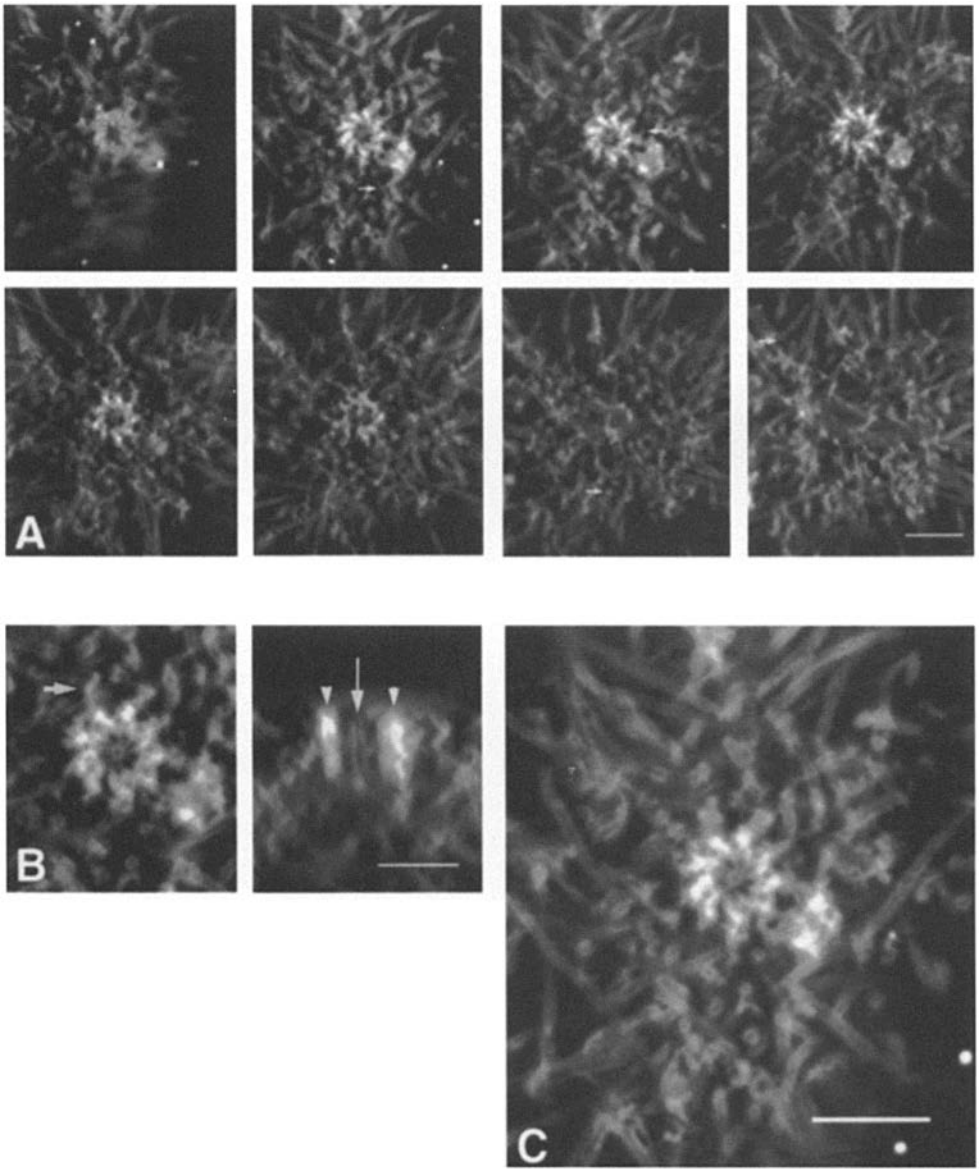

Figure 4. Selected views (from a total of 120) from a three-dimensional reconstruction of the centrosome shown in Fig 4 *a*. (*a*) A series of selected views stepping through the centrosome are shown; each step represents 22.5 nm. Arrows mark minus ends of 4 MTs. In panels *2*, *3*, and *8* (counting from left to right, beginning with upper left) the MTs marked by the arrow extend towards the "1 or 2 o'clock" position with respect to the arrowhead. The MT whose minus end is marked in panel 7 cannot be seen because it extended toward the viewer. Note the centriole pair at the center of some views. White dots visible in some views are 15-nm gold beads used as fiducial markers for alignment. (*b*) Enlarged views of centrioles. (*Left*) Transverse view of a centriole showing the ring of nine singlet MTs surrounding a central tubule, and the spokes spanning the gap between the two structures. Arrow marks an electron-dense structure extending outward from a MT in the ring. (*Right*) Enlarged longitudinal view of the same centriole shown in transverse view in the left-hand panel. This longitudinal view shows that the central tubule spans the length of the centriole (*arrow*). Arrowheads mark the walls of the centriole. (*c*) 0° view enlarged to show detail. Bars: (*a* and *c*) 200 nm; (*b*) 135 nm.

dense material extends outward from each MT in the ring (see arrow Fig. 4 *b*). The length of the centriole cylinder shown here in longitudinal section is ~80 nm, but the centrioles of other centrosomes vary in length, up to ~180 nm (data not shown). In general, it appears that the centrioles of the early *Drosophila* embryo are significantly shorter than mammalian centrioles, which range from ~175–700 nm in length (for example see Wheatley, 1982). The diameter of the *Drosophila* centriole is ~160–200 nm, which is comparable to that of a mammalian centriole.

In this particular centrosome, the PCM is ~800 nm in diameter. MTs appear to criss-cross the PCM in a random fashion (Fig. 4). This aspect of centrosome structure can be appreciated best by viewing stereo pairs generated from 10 sections of the reconstruction (Fig. 5). Note that MTs sometimes originate on one side of the centrosome but project back inward and across the PCM before emerging outward on the other side. In other words, MTs do not always take the shortest route outward from the centrosome.

Perhaps most interestingly, by following individual MTs through the three-dimensional reconstruction, it was possible to identify unambiguously origins for 36 MTs. We can assume that these are the minus and not the plus ends of MTs based on previous work on the centrosomes of mammalian cells (Bergen et al., 1980). A model that represents the MTs that were followed through the reconstruction provides a schematic view of their arrangement (Fig. 6). Significantly, there is no large structure apparent at the minus ends of MTs; the MTs appear to arise abruptly, suggesting that if there is a nucleating structure physically contacting the MT, it must conform closely to the shape of the MT (see Fig. 4 *a, arrows*). Although unlikely, we cannot rule out the possibility that all 36 MT minus ends have been released from their actual nucleating sites and have moved away (see Discussion).

In an effort to look for a regular pattern of MT origins within the PCM, the distances (closest approach) between the minus ends of these 36 MTs and the centrioles were measured. A histogram of these distances shows that MTs

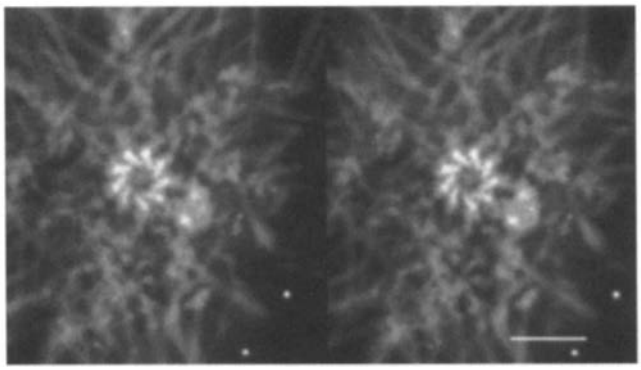

Figure 5. A stereo pair generated from 10 sections of the reconstruction of a centrosome illustrates that MTs cross through the PCM in all directions, suggesting that the nucleating sites are oriented in many directions. Bar, 200 nm.

originate between ~20 and 220 nm from their nearest centriole in this centrosome with a PCM diameter of ~800 nm (Fig. 7). This suggests that nucleating sites are distributed throughout the PCM and are not tightly confined to one region. However, minus ends do appear to be more prevalent in the region within ~80 nm from the centrioles. If the distribution of nucleating sites were completely random within the PCM, one would expect their numbers to increase linearly or quadratically with the distance from the centrioles due to the radial dependence of the shell volume (cylindrical or spherical), which is not what we observe.

The centrosome chosen for reconstruction contains perhaps hundreds of MTs (Fig. 2 *a*), and the 36 MTs whose minus ends we were able to identify unambiguously are likely to represent perhaps 15% of the total number. Our failure to identify the origins of the majority of MTs was not due to their being buried in amorphous, electron dense material, but to the close and complicated packing of MTs against each other causing uncertainty in the precise location of the ends. Thus, we believe that the 36 MT origins discussed here are representative of the MT minus ends within the centrosome.

We also explored the possibility that some discernible structural order exists within the PCM by reconstructing a centrosome without regrown MTs. Two remarkable features emerged with this reconstruction that have not been revealed previously by conventional EM studies of the centrosome. First, to our surprise, the PCM in this "naked" centrosome appears much more dense and prominent than the PCM in the centrosome with MTs (compare Figs. 4 and 8). This difference in PCM density is also apparent in the raw data used for these two reconstructions (compare Figs. 2 *c* and 8 *a*). Reconstructions of two additional naked centrosomes confirms this conclusion (data not shown). Although the density of the PCM varies from centrosome to centrosome both with and without MTs present, the extreme density of PCM seen in naked centrosomes is never seen in the presence of MTs (Figs. 2 and 8 and data not shown).

The second striking feature brought out by the reconstruction of the naked centrosome is the existence of numerous small ring-like structures dispersed throughout the PCM (Fig. 8, *b* and *c*, *white arrows*). These rings have a diameter of ~25–30 nm and a length of ~10–13 nm ($n = 10$). Stepping through all projections in the reconstruction data set shows that the rings can be found at all levels in the PCM (examples of two projections are shown in Fig. 8, *b* and *c*), and that they are oriented in all directions. Finally, in addition to the ring structures, the PCM consists of fibrous material that is interspersed with apparently empty channels. The possible significance of the variation in PCM density and the ring structures is considered in the Discussion.

The reconstruction of the naked centrosome again shows that the centrioles consist of a ring of nine singlet MTs surrounding a central tubule and that the ring and the central tubule are connected by nine spokes (Fig. 8). The dimensions of the centriole shown longitudinally in Fig. 8

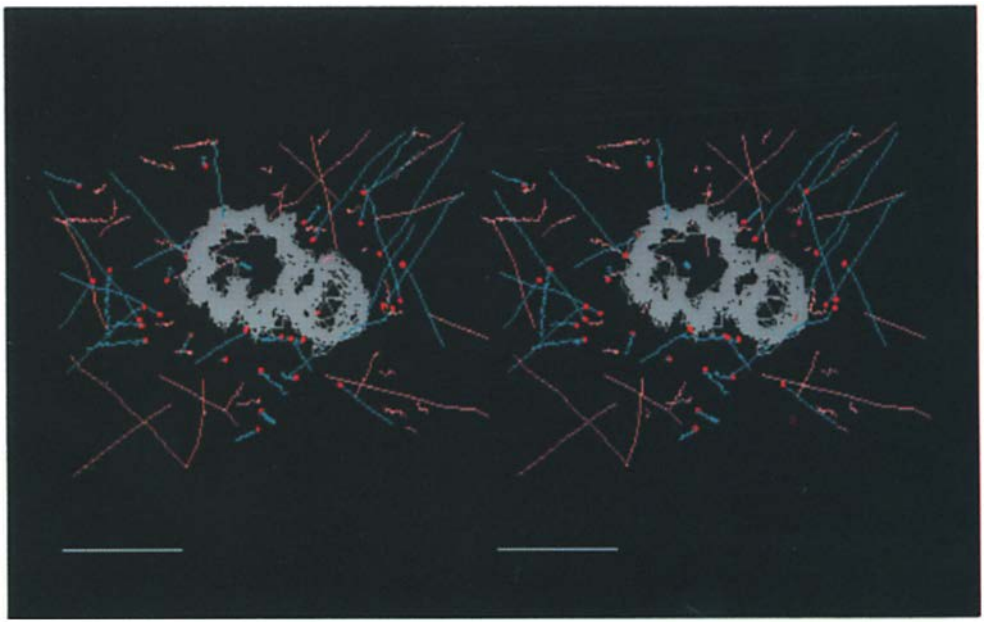

Figure 6. Drawing of a centrosome reconstruction. A stereo pair of a model illustrating 36 MTs (*blue*) that could be followed to their minus ends (*red dots*). MT minus ends are concentrated near the centrioles (*grey*), but some are also found farther away. MTs whose minus ends were uncertain are shown in pink. Bar, 200 nm.

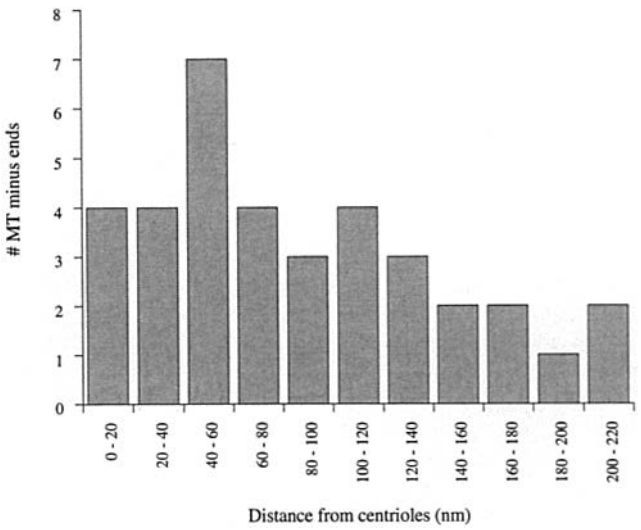

Figure 7. The spatial distribution of MT minus ends within the PCM. MT minus ends are distributed throughout the PCM, but appear to be concentrated nearer the centrioles. A plot of distances between MT origins and the nearest centriole wall versus the number of MT ends is shown.

are ~150 nm long by ~150 nm wide. The other centriole is ~200 nm wide, including the extensions on the ring of MTs. These two centrioles are quite far apart, suggesting that this centrosome was beginning to duplicate upon isolation (compare distances between centrioles in Fig. 4 and 8).

Note that there are regularly spaced connections between the central tubule and the outer wall of the centriole in longitudinal view (Fig. 8 *b, black arrow*). These may be the same "spokes" that are visible in the transverse view, indicating that the spokes are not solid structures that extend from one end of the centriole to the other, but are instead a series of rung-like projections.

Discussion

Electron tomography of isolated centrosomes has allowed us to reconstruct a three-dimensional image of the PCM with and without its associated MTs. By following individual MTs through the reconstruction we were able to map unambiguously the minus ends of 36 MTs. These data indicate that while MTs can nucleate throughout the PCM, there is a preference for nucleating sites to be closer to the centrioles (Fig. 7). Significantly, no large structure is visible at the origins of MTs (Figs. 4 and 5), suggesting that the nucleation structure must conform closely to the MT minus end. Alternatively, the MTs whose minus ends we can identify may no longer be associated with nucleating sites. It has been proposed that MTs may be nucleated, released, and recaptured by the centrosome (Harris et al., 1980; Kitanishi-Yumura and Fukui, 1987; Ault and Nicklas, 1989; Belmont et al., 1990). However, we did not find any MT minus ends buried in large electron-dense areas, as might be expected if MTs can exist in the two states: associated or dissociated from nucleating sites.

The orientation of MT-nucleating sites with respect to the surface of the PCM appears to be random (Figs. 4 and 5): in some cases MTs are observed to originate on one side of the centrosome and instead of growing along the shortest path outward, they traverse the PCM and emerge from it on the opposite side of the centrosome. However, because the asters were centrifuged onto Thermonox disks before fixation and embedding for EM, it is possible that the arrangement of the MTs within the PCM could have been altered by the force of the centrifugation. We consider it unlikely, though, that gross rearrangements of the MTs have occurred given that the MTs are projecting in all directions as they do in the cell. In addition, a relatively low centrifugal force was used (23,000 *g* for 10 min through 30% glycerol), and the asters were fixed before sedimentation.

The reconstruction of a centrosome without MTs (Fig. 8) reveals two intriguing features that were not apparent previously from conventional EM studies of the centrosome: a different appearance of the PCM in centrosomes with and without MTs, and ring-like structures within the PCM. We suggest that the PCM may become redistributed as MTs grow out of it, making it less discernible in our reconstructions of centrosomes with MTs. For instance, proteins of the PCM could distribute themselves along part of the length of the MTs within the centrosome. A similar scenario has been proposed to explain the apparent disappearance of the fibrous corona of kinetochores when they are associated with MTs (Rieder, 1982, 1990). Of course it is also possible that the PCM in centrosomes with and without MTs appears to be different because of differences in our ability to fix them, or the ability of EM stains to penetrate the MTs. However, since these same fixatives and stains are able to penetrate specimens that are much more dense, such as whole cells, embryos, and tissues, we consider these possibilities unlikely. Nevertheless, in the future it will be worth attempting to compare the PCM in centrosomes with and without MTs using EM techniques, such as freeze substitution, that are thought to preserve structure better.

Strikingly, reconstructions of centrosomes without MTs reveal numerous ring-like structures throughout the PCM. These rings are found at every level of the PCM and they appear to be oriented in all directions. The diameter of these rings is approximately the same as that of a MT and their thickness is ~10–13 nm. It is unlikely that the rings represent residual MTs that were not completely depolymerized during the centrosome isolation procedure, because in this case, the thickness of the rings should be more heterogeneous. A more intriguing possibility is that the rings are MT-nucleating structures, consistent with the appearance of MT minus ends shown in Fig. 4.

The reconstructions also reveal that early embryonic *Drosophila* centrioles consist of a ring of nine singlet MTs surrounding a central tubule, whose dimensions suggest that it is also a MT. Immuno-EM using antisera against α- or β-tubulin will be necessary to confirm this. Nine radial spokes appear to connect the central tubule with the outer ring through a series of rungs. Nine structures extend outward from the ring, showing that the MTs of the centriole are not naked, but are decorated with associated proteins.

These centrioles are considerably shorter (80–180 vs. 175–700 nm) than mammalian centrioles (Figs. 4 and 8). Their appearance is reminiscent of newly forming mammalian centrioles, which begin with a ring of singlet MTs

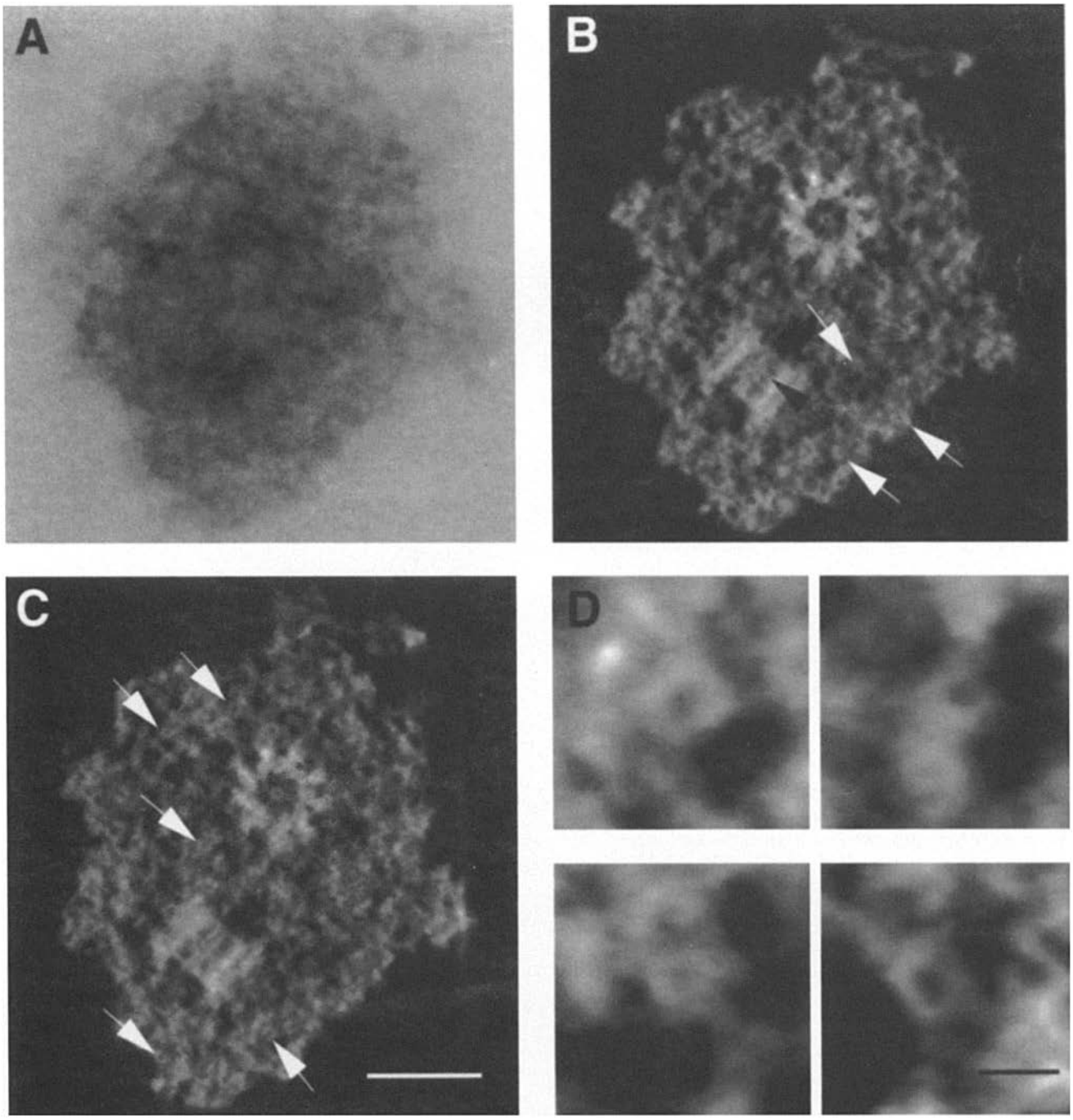

Figure 8. Reconstruction of a centrosome without MTs. (*a*) An example of raw data used for the reconstruction shown in *b* and *c*. Note that the PCM is more dense in appearance than the PCM in Fig. 2 *a*. (*b* and *c*) Examples of two projections from the reconstruction of a centrosome without MTs. Each projection represents a 2.7-nm slice through the centrosome. The projections shown are 8.1 nm apart. White arrows mark examples of ring-like structures. Additional rings are visible throughout the PCM. The black arrow marks thin projections between the outer wall of the centriole and the central tubule. (*d*) Enlarged view of rings within the PCM. Bars: (*a–c*) 200 nm; (*d*) 28 nm.

surrounding a central "hub" with "spokes." As mammalian centrioles grow they acquire triplet MTs and ultimately the central hub and spokes appear to deteriorate. It has been suggested that this "cartwheel" structure provides stability to the newly growing centriole (reviewed in Vorobjev and Nadezhdina, 1987; Wheatley, 1982).

The paedomorphic (juvenile in form) nature of the *Drosophila* centriole might reflect the rapid (8–10 min) mitoses of the early embryo; perhaps there is only enough time in each mitosis to build a minimal centriole. If so, the embryonic centriole may consist of the minimal requirements for function. In support of this, more mature *Drosophila* cells, which divide more slowly, contain centrioles with doublet and triplet MTs. In these cells the internal

cartwheel is sometimes still visible (Mahowald and Strassheim, 1970; Tucker et al., 1986; Callaini and Anselmi, 1988; Marcaillou et al., 1993). Unfortunately, one cannot determine the length of the centriole in more mature *Drosophila* cells from these earlier studies. Although some previous investigators have concluded that early (precellular blastoderm) embryonic centrioles consist of triplet MTs, in our opinion their micrographs appear to show singlets surrounding the cartwheel in agreement with our data (Callaini and Anselmi, 1988; Callaini and Riparbelli, 1990). In addition, K. McDonald (University of California, Berkeley) has concluded that these centrioles consist of singlet MTs based on serial thin section EM studies of embryos (unpublished observations and personal communication). A particularly nice example of a thin section through an early embryonic centriole that clearly shows the ring of nine singlets surrounding a central tubule has been published in McDonald and Morphew (1993).

Using electron tomography and antibodies against known centrosomal proteins such as γ-tubulin, CP60 and CP190, we should now be able to map the positions of these proteins with respect to the minus ends of MTs with high resolution, as well as to study cell cycle- and MT-dependent structural changes within the PCM. For example, it has been proposed that γ-tubulin molecules are situated at the minus ends of each protofilament within a MT (Oakley, 1992). It should be possible to confirm or disprove this hypothesis by immunogold labeling of γ-tubulin followed by tomography. Moreover, if the rings seen in Fig. 8 are MT-nucleating structures, they should stain with antibodies against γ-tubulin. Such approaches should provide additional insight into the longstanding mystery of MT nucleation by the centrosome.

The authors made the following contributions to this study: M. Moritz, in the laboratory of B. M. Agard, developed the centrosome isolation protocol, prepared samples for EM, and interpreted the data. M. B. Braunfeld prepared samples for the tomography, collected EM data, calculated the reconstructions and modeled the data for analysis. J. C. Fung participated in the reconstructions and made major contributions to the development of the automated EM tomography system with J. W. Sedat and D. A. Agard. We thank L. Evans for expert and friendly advice on centrosome EM, T. Stearns for helpful discussions in the initial stages of this project, and H. Chen, D. Diggs, and W. Liu for help with computer programs. We thank R. Aroian, B. Kellum, T. Mitchison, K. Oegema, and Y. Zheng for many fruitful discussions and critical readings of the manuscript.

M. Moritz was supported by a postdoctoral fellowship from the American Cancer Society. This work was supported by the Howard Hughes Medical Institute (J. W. Sedat and D. A. Agard), and National Institutes of Health grants GM31627 (D. A. Agard), GM23928 (B. M. Alberts), and GM25101 (J. W. Sedat).

Received for publication 3 May 1995 and in revised form 18 May 1995.

References

Alieva, I. B., E. S. Nadezhdina, E. A. Vaisberg, and I. A. Vorobjev. 1992. Microtubule and intermediate filament patterns around the centrosome in interphase cells. *In* The Centrosome. V. I. Kalnins, editor. Academic Press, San Diego. 103–129.

Ashburner, M. 1989. *Drosophila*, a laboratory handbook. Cold Spring Harbor Laboratory Press, Cold Spring Harbor. 216 pp.

Ault, J. G., and R. B. Nicklas. 1989. Tension, microtubule rearrangements, and the proper distribution of chromosomes in mitosis. *Chromosoma.* 98:33–39.

Belmont, A. S., J. W. Sedat, and D. A. Agard. 1987. A three-dimensional approach to mitotic chromosome structure: evidence for a complex hierarchical organization. *J. Cell Biol.* 105:77–92.

Belmont, L. D., A. A. Hyman, K. E. Sawin, and T. J. Mitchison. 1990. Real-time visualization of cell cycle-dependent changes in microtubule dynamics in cytoplasmic extracts. *Cell.* 62:579–589.

Bergen, L. G., R. Kuriyama, and G. G. Borisy. 1980. Polarity of microtubules nucleated by centrosomes and chromosomes of chinese hamster ovary cells in vitro. *J. Cell Biol.* 84:151–159.

Bozzola, J. J., and L. D. Russell. 1992. Electron microscopy: principles and techniques for biologists. Jones and Bartlett, Boston. 390–394.

Braunfeld, M. B., A. J. Koster, J. W. Sedat, and D. A. Agard. 1994. Cryo automated electron tomography: towards high-resolution reconstructions of plastic-embedded structures. *J. Microsc. (Oxf.).* 174:75–84.

Brinkley, B. R., S. M. Cox, D. A. Pepper, L. Wible, S. L. Brenner, and R. L. Pardue. 1981. Tubulin assembly sites and the organization of cytoplasmic microtubules in cultured mammalian cells. *J. Cell Biol.* 90:554–562.

Byers, B., K. Shriver, and L. Goetsch. 1978. The role of spindle pole bodies and modified microtubule ends in the initiation of microtubule assembly in *Saccharomyces cerevisiae*. *J. Cell Sci.* 30:331–352.

Callaini, G., and F. Anselmi. 1988. Centrosome splitting during nuclear elongation in the *Drosophila* embryo. *Exp. Cell Res.* 178:415–425.

Callaini, G., and M. G. Riparbelli. 1990. Centriole and centrosome cycle in the early *Drosophila* embryo. *J. Cell Sci.* 97:539–543.

Chen, H., J. W. Sedat, and D. A. Agard. 1990. Manipulation, display, and analysis of three-dimensional biological images. *In* Handbook of Biological Confocal Microscopy. J. Pawley, editor. Plenum Press, NY. 141–150.

Chen, H., W. Clyborne, J. W. Sedat, and D. A. Agard. 1992. PRISM: an integrated system for display and analysis of three-dimensional microscope images. *SPIE: Biomedical Image Processing and Three-Dimensional Microscopy.* 1660:784–790.

Evans, L., T. Mitchison, and M. Kirschner. 1985. Influence of the centrosome on the structure of nucleated microtubules. *J. Cell Biol.* 100:1185–1191.

Felix, M.-A., C. Antony, M. Wright, and B. Maro. 1994. Centrosome assembly in vitro: role of γ-tubulin recruitment in *Xenopus* sperm aster formation. *J. Cell Biol.* 124:19–31.

Frank, J. 1992. Introduction: principles of electron tomography. *In* Electron tomography: three-dimensional imaging with the transmission electron microscope. J. Frank, editor. Plenum Press, NY. 1–13.

Frank, J., B. F. McEwen, M. Radermacher, J. N. Turner, and C. F. Rieder. 1987. Three-dimensional tomographic reconstruction in high voltage electron microscopy. *J. Electron Microsc. Tech.* 6:193–205.

Gould, R. R., and G. G. Borisy. 1977. The pericentriolar material in Chinese hamster ovary cells nucleates microtubule formation. *J. Cell. Biol.* 73:601–615.

Harris, P., M. Osborn, and K. Weber. 1980. Distribution of tubulin-containing structures in the egg of sea urchin *Strongylocentrotus purpuratus* from fertilization through first cleavage. *J. Cell Biol.* 84:668–678.

Horio, T., S. Uzawa, M. K. Jung, B. R. Oakley, K. Tanaka, and M. Yanagida. 1991. The fission yeast γ-tubulin is essential for mitosis and is localized at microtubule organizing centers. *J. Cell Sci.* 99:693–700.

Hyatt, M. A. 1981. Principles and techniques of electron microscopy-biological applications. Vol. 1. University Park Press, Baltimore. 161 pp.

Hyman, A., D. Drechsel, D. Kellogg, S. Salser, K. Sawin, P. Steffen, L. Wordeman, and T. Mitchison. 1991. Preparation of modified tubulins. *Methods Enzymol.* 196:478–487.

Joshi, H. C., M. J. Palacios, L. McNamara, and D. W. Cleveland. 1992. γ-tubulin is a centrosomal protein required for cell cycle-dependent microtubule nucleation. *Nature (Lond.).* 356:80–83.

Kalnins, V. I., Editor. 1992. The Centrosome. Academic Press, San Diego. 368 pp.

Kalt, A., and M. Schliwa. 1993. Molecular Components of the Centrosome. *Trends Cell Biol.* 3:119–128.

Kellogg, D. R., and B. M. Alberts. 1992. Purification of a multiprotein complex containing centrosomal proteins from the *Drosophila* embryo by chromatography with low-affinity polyclonal antibodies. *Mol. Biol. Cell.* 3:1–11.

Kellogg, D. R., T. J. Mitchison, and B. M. Alberts. 1988. Behaviour of microtubules and actin filaments in living *Drosophila* embryos. *Development (Camb.).* 103:675–686.

Kellogg, D. R., M. Moritz, and B. M. Alberts. 1994. The centrosome and cellular organization. *Annu. Rev. Biochem.* 63:639–674.

Kitanishi-Yumura, T., and Y. Fukui. 1987. Reorganization of microtubules during mitosis in *Dictyostelium:* dissociation from MTOC and selective assembly/disassembly in situ. *Cell Mot. Cytoskeleton.* 8:106–117.

Koster, A. J., H. Chen, J. W. Sedat, and D. A. Agard. 1992. Automated microscopy for electron tomography. *Ultramicroscopy.* 46:207–227.

Koster, A. J., M. B. Braunfeld, J. Fung, C. K. Abbey, K. F. Han, W. Liu, H. Chen, J. W. Sedat, and D. A. Agard. 1993. Towards automatic three-dimensional imaging of large biological structures using intermediate voltage electron microscopy. *Microsc. Soc. Am. Bull.* 23:176–188.

Kuriyama, R. 1984. Activity and stability of centrosomes in chinese hamster ovary cells in nucleation of microtubules *in vitro*. *J. Cell Sci.* 66:277–295.

Lawrence, M. C. 1983. Alignment of images for three-dimensional reconstructions of non-periodic objects. *Proc. Electron Microsc. Soc. S. Africa.* 13:19–20.

Mahowald, A. P., and J. M. Strassheim. 1970. Intercellular migration of centrioles in the germarium of *Drosophila* melanogaster. *J. Cell Biol.* 45:306–320.

Marcaillou, C., A. Debec, S. Lauverjat, and A. Saihi. 1993. The effect of the heat shock response on ultrastructure of the centrosome of *Drosophila* cultured cells in interphase: possible relation with changes in the chemical state

of calcium. *Biochem. Cell Biol.* 71:507–517.
McDonald, K., and M. K. Morphew. 1993. Improved preservation of ultrastructure in difficult-to-fix organisms by high pressure freezing and freeze substitution: I. *Drosophila melanogaster* and *Strongylocentrotus purpuratus* embryos. *Microscopy Res. and Tech.* 24:465–473.
McEwen, B. F., J. T. Arena, J. Frank, and C. L. Rieder. 1993. Structure of the colcemid-treated PtK1 kinetochore outer plate as determined by high-voltage electron microscopic tomography. *J. Cell Biol.* 120:301–312.
Minden, J. S., D. A. Agard, J. W. Sedat, and B. M. Alberts. 1989. Direct cell lineage analysis in *Drosophila melanogaster* by time-lapse, three-dimensional optical microscopy of living embryos. *J Cell Biol.* 109:505–516.
Mitchison, T. J., and M. W. Kirschner. 1984. Microtubule assembly nucleated by isolated centrosomes. *Nature (Lond.).* 312:232–237.
Oakley, B. R. 1992. γ-Tubulin: the microtubule organizer? *Trends Cell Biol.* 2: 1–5.
Oakley, B. R., C. E. Oakley, Y. Yoon, and M. K. Jung. 1990. γ-Tubulin is a component of the spindle pole body that is essential for microtubule function in *Aspergillus nidulans. Cell.* 61:1289–1301.
Olins, A. L. 1986. Electron microscope tomography: 3D reconstruction of asymmetric structures. *Proc. 44th Annu. Electron Microsc. Soc. Amer.* 22–55.
Raff, J. W., D. R. Kellogg, and B. M. Alberts. 1993. *Drosophila* γ-tubulin is part of a complex containing two previously identified centrosomal MAPs. *J. Cell Biol.* 121:823–835.
Rattner, J. B. 1992. Ultrastructure of centrosome domains and identification of their protein components. *In* The Centrosome. V. I. Kalnins, editor. Academic Press, San Diego. 45–64.
Rieder, C. L. 1982. The formation, structure, and composition of the mammalian kinetochore and kinetochore fiber. *Int. Rev. Cytol.* 79:1–58.
Rieder, C. L. 1990. Kinetochores are transported poleward along a single astral microtubule during chromosome attachment to the spindle in newt lung cells. *J. Cell Biol.* 110:81–95.
Scheele, R. B., L. F. Bergen, and G. G. Borisy. 1982. Control of structural fidelity of microtubules by initiation sites. *J. Cell Biol.* 154:485–500.
Skoglund, U., K. Andersson, B. Strandberg, and B. Daneholt. 1986. Three-dimensional structure of a specific premessenger RNP particle established by electron microscope tomography. *Nature (Lond.).* 319:560–564.
Stearns, T., and M. Kirschner. 1994. In vitro reconstitution of centrosome assembly and function: the role of γ-tubulin. *Cell.* 76:623–637.
Stearns, T., L. Evans, and M. Kirschner. 1991. γ-Tubulin is a highly conserved component of the centrosome. *Cell.* 65:825–836.
Tilney, L. G., J. Bryan, D. J. Bush, K. Fujiwara, M. Mooseker, D. B. Murphy, and D. H. Snyder. 1973. Microtubules: evidence for 13 protofilaments. *J. Cell Biol.* 59:267–275.
Tucker, J. B., M. J. Milner, D. A. Currie, J. W. Muir, D. A. Forrest, and M. J. Spencer. 1986. Centrosomal microtubule-organizing centres and a switch in the control of protofilament number for cell surface-associated microtubules during *Drosophila* wing morphogenesis. *Eur. J. Cell Biol.* 41:279–289.
Vorobjev, I. A., and E. S. Nadezhdina. 1987. The centrosome and its role in the organization of microtubules. *Int. Rev. Cytol.* 106:227–293.
Wheatley, D. N. 1982. The Centriole: A Central Enigma of Cell Biology. Elsevier Biomedical Press, NY. 232 pp.
Whitfield, W. G., S. E. Millar, H. Saumweber, M. Frasch, and D. M. Glover. 1988. Cloning of a gene encoding an antigen associated with the centrosome in *Drosophila. J. Cell Sci.* 89:467–480.
Zheng, Y., M. K. Jung, and B. R. Oakley. 1991. γ-Tubulin is present in *Drosophila melanogaster* and *Homo sapiens* and is associated with the centrosome. *Cell.* 65:817–823.